A R C H I V E O F M E C H A N I C A L E N G I N E E R I N G

VOL. LXI 2014 Number 4

10.2478/meceng-2014-0035

Key words: railway vehicle, vertical vibration, critical points track irregularity, comfort index

MĂDĂLINA DUMITRIU *

ON THE CRITICAL POINTS OF VERTICAL VIBRATION IN A RAILWAY VEHICLE

This paper evaluates the level of the vertical vibrations in a railway vehicle carbody generated by the track irregularities and examines the position of the critical point from the comfort perspective. The issue is reviewed on the basis of both a „rigid carbody" model and a „flexible carbody" model, which considers the first two carbody bending modes. The model errors are calculated as a function of the speed behaviour, and the results prove that the comfort performance of a railway vehicle evaluated on the „rigid carbody" model basis are overestimated compared to the ones derived from the implementation of the „flexible carbody" model, mainly at the centre of the carbody. Similarly, a correct estimation of the critical point position in the level of vibrations requires the modelling of the structural vibrations of the vehicle carbody.

1. Introduction

While running, the railway vehicle is subjected to a permanent vibrations behaviour, mainly developed by the geometrical defects of the track [1]. The evaluation of the vibration behaviour is essential, even since the designing stage, so as to predict the dynamic behaviour of the railway vehicle and select the optimum designing parameters that will lead to the best performance of the vehicle.

The study of the vertical vibrations of the railway vehicles requires the adopting of certain complex models, especially when the comfort performance is evaluated in the vehicle of high speed [2-8]. The results derived from the simple models of „rigid body" type show that the critical position in terms of comfort is at the carbody ends, since the vertical movement here is the effect of the overlapping of the pitch and bounce vibrations, unlike the

* *Department of Railway Vehicles, University Politehnica of Bucharest, Bucharest, Romania; E-mail: madalinadumitriu@yahoo.com*

Unauthenticated
Download Date | 1/13/15 10:38 AM

carbody centre where the bounce only is present [3]. This fact is not often the image of reality, as there are cases where the level of vibration at the carbody centre is comparable with the level of vibration recorded at both ends or even higher, as shown in this paper. The explanation is that both the vibration rigid modes of the vehicle and the flexible ones are excited while running over the geometrical irregularities of the track, which leads to an increase in the level of vibrations inside the vehicle carbody, mainly at high velocities. The numerical and experimental studies [4-6] have indeed proved that the running confort at the high speed trains can be influenced by the resonance phenomenon of the carbody flexible vibration modes. Even though the carbody structural vibrations are rather complex [2, 9], the greatest influence upon the vehicle vertical vibrations comes from the first flexible vibration mode of the carbody, which have the frequency ranging from 7 to 12 Hz [4-6].

This paper evaluates the level of the vertical vibrations in a railway vehicle carbody generated by the track irregularities. For this purpose, the comfort index is calculated in three reference points of the carbody – at the centre and above the two bogies [10, 11]. The concept of critical point of the level of vibrations is being here introduced, as the reference point of the carbody where the running comfort is the least favorable [7] and its position is being examined, depending on the running behaviour and the suspension damping. The issue is being looked at via a „flexible carbody" model that considers both the rigid modes of the carbody vibration and its first two flexible modes and the results are compared with the ones derived from the carbody modelling as a rigid body.

2. The mechanical model and the vehicle movement equations

The vehicle is represented by a mechanical model with 10 degrees of freedom, which contains a body with distributed parameters for the carbody and 6 rigid bodies representing the bogies and the axles, connected among them by Kelvin-Voigt systems to help modelling the two levels of suspension (Fig. 1).

The vehicle carbody is modelled by an uniform Euler-Bernoulli beam of length L, with the mass per unit length ρ_c and the bending module EI. The first two natural carbody bending modes are taken into account, in a vertical plan (symmetrical and antisymmetrical), as well as the rigid vibration modes in the carbody, namely the bounce z_c and pitch θ_c. The carbody inertia compared to the rigid vibration modes is represented by the mass $m_c = \rho_c L$ and the inertia moment J_c.

Unauthenticated
Download Date | 1/13/15 10:38 AM

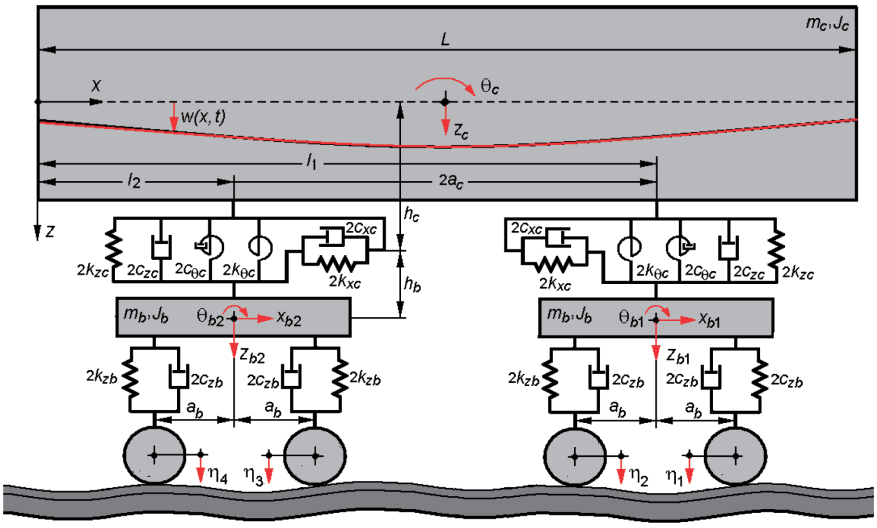

Fig. 1. The mechanical model of the vehicle

The carbody displacement $w(x,t)$ is the result of overlapping the rigid vibration modes with the bending ones

$$w(x,t) = z_c(t) + \left(x - \frac{L}{2}\right)\theta_c(t) + \sum_{n=2}^{3} X_n(x)T_n(t), \tag{1}$$

where $T_n(t)$, with $n = 2, 3$, is the coordinate of the natural bending mode n, and $X_n(x)$, is the eigenfunctions of the first two carbody vertical bending modes

$$X_n(x) = \sin\beta_n x + \sinh\beta_n x - \frac{\sin\beta_n L - \sinh\beta_n L}{\cos\beta_n L - \cosh\beta_n L}(\cos\beta_n x + \cosh\beta_n x), \tag{2}$$

with

$$\beta_n = \sqrt{\omega_n^2 m/(EI)} \tag{3}$$

and

$$\cos\beta_i L \cosh\beta_i L - 1 = 0. \tag{4}$$

where ω_n is the angular natural pulsation of the vibration mode n.

The stiffness, damping and the modal mass of the carbody are given by the equations below

$$k_{mn} = EI\int_0^L \left(\frac{\mathrm{d}^2X_n}{\mathrm{d}x^2}\right)^2 \mathrm{d}x;\ c_{mn} = \mu I\int_0^L \left(\frac{\mathrm{d}^2X_n}{\mathrm{d}x^2}\right)^2 \mathrm{d}x;\ m_{mn} = \rho_c\int_0^L X_n^2\,\mathrm{d}x,\ \text{for } n = 2, 3, \tag{5}$$

Unauthenticated
Download Date | 1/13/15 10:38 AM

where E is the longitudinal elasticity module, I – the inertia moment of the beam transversal section, and μ – the carbody coefficient of structural damping.

The bogies are considered as rigid bodies with three degrees of freedom, with the following movements: bounce z_{bi}, rebound x_{bi} and pitch θ_{bi}, with $i = 1, 2$. The bogie mass is m_b, and the inertia moment is J_b.

The primary suspension corresponding to an axle is modelled via a Kelvin-Voigt system, which operates on translation in a vertical direction, with the elastic constant $2k_{zb}$, and the damping constant $2c_{zb}$. The modelling of the secondary suspension pertinent to a bogie is done by means of three Kelvin-Voigt systems, two for translation (vertical and longitudinal) and one for rotation. The Kelvin-Voigt system, placed at the distance h_c from the carbody neutral axis and at the distance h_b from the bogie's centre of gravity models the transmission system of the longitudinal forces between the carbody and the bogie. The features of the secondary suspension are represented by the elastic components in the vertical direction $2k_{zc}$, longitudinal $2k_{xc}$ and the angle stiffness of pitch $2k_{\theta c}$, as well as by the damping constants $2c_{zc}$, $2c_{xc}$ and $2c_{\theta c}$.

The hypothesis of a perfectly rigid track with nivelment irregularities has been adopted, which imprints displacements in a vertical plan to the vehicle, via the axles. The nivelment irregularities, with wavelength Λ and amplitude η_0 are described by the functions $\eta_{j,(j+1)}$, with $j = 2i - 1$, for $i = 1, 2$, while mentioning that every bogies is fitted with the axles j and $j+1$. For those four axles, these functions are in the following form

$$\eta_{1,2}(t) = \eta_0 \cos \frac{2\pi V}{\Lambda}\left(t + \frac{a_c \pm a_b}{V}\right); \ \eta_{3,4}(x) = \eta_0 \cos \frac{2\pi V}{\Lambda}\left(t - \frac{a_c \mp a_b}{V}\right), \quad (6)$$

where V is the vehicle speed, $2a_c$ represents the carbody wheelbase and $2a_b$ – the bogie wheelbase.

The carbody movement equation writes as below

$$EI\frac{\partial^4 w(x,t)}{\partial x^4} + \mu I\frac{\partial^5 w(x,t)}{\partial x^4 \partial t} + \rho_c \frac{\partial^2 w(x,t)}{\partial t^2} = \sum_{i=1}^{2} F_{zci}\delta(x - l_i) - \sum_{i=1}^{2}(M_{ci} - h_c F_{xci})\frac{\mathrm{d}\delta(x - l_i)}{\mathrm{d}x}, \quad (7)$$

where $\delta(.)$ is Dirac delta function, the distances l_i fix the position of the leaning points of the carbody on the secondary suspension, and F_{xci}, F_{zci} and M_i are the forces and the moments due to the secondary suspension of the bogie i

$$F_{zci} = -2c_{zc}\left(\frac{\partial w(l_i,t)}{\partial t} - \dot{z}_{bi}\right) - 2k_{zc}\left[w(l_i,t) - z_{bi}\right]; \quad (8)$$

Unauthenticated
Download Date | 1/13/15 10:38 AM

$$M_{ci} = -2c_{\theta c}\left(\frac{\partial^2 w(l_i,t)}{\partial x \partial t} - \dot{\theta}_{bi}\right) - 2k_{\theta c}\left[\frac{\partial w(l_i,t)}{\partial x} - \theta_{bi}\right]; \tag{9}$$

$$F_{xci} = 2c_{xc}\left(h_c\frac{\partial^2 w(l_i,t)}{\partial x \partial t} + \dot{x}_{bi} + h_b\dot{\theta}_{bi}\right) + 2k_{xc}\left(h_c\frac{\partial w(l_i,t)}{\partial x} + x_{bi} + h_b\theta_{bi}\right). \tag{10}$$

The equations defining the movement of bounce, pitch and rebound of the bogies are:

$$m_b\ddot{z}_{bi} = \sum_{j=2i-1}^{2i} F_{zbj,(j+1)} - F_{zci}, \text{ with } i = 1,2 \text{ and } j = 2i-1; \tag{11}$$

$$J_b\ddot{\theta}_{bi} = a_b\sum_{j=2i-1}^{2i}(-1)^{j+1}F_{zbj} - M_{ci} - h_bF_{xci}, \text{ with } i = 1,2 \text{ and } j = 2i-1; \tag{12}$$

$$m_b\ddot{x}_{bi} = F_{xci}, \text{ with } i = 1,2, \tag{13}$$

where $F_{zbj,(j+1)}$, i.e the forces derived from the primary suspension of the axles j, and $(j+1)$ respectively

$$F_{zbj,(j+1)} = -2c_{zb}(\dot{z}_{bi} \pm a_b\dot{\theta}_{bi} - \dot{\eta}_{oj,(j+1)}) - 2k_{zb}(z_{bi} \pm a_b\theta_{bi} - \eta_{oj,(j+1)}). \tag{14}$$

Upon implementing the method of the modal analysis, the carbody movement equation that includes partial derivatives is turned into equations with ordinary derivatives that describe the movements of bounce, pitch and the symmetrical and antisymmetrical bending of the carbody. Hence, the vehicle vibrations are defined by a system of 10 coupled equations. The solving of these equations is simpler provided that their decoupling is achieved [12] by means of an appropriate processing. For this purpose, the parameters of the symmetrical movements are written as

$$p_1^+ = z_c;\ p_2^+ = T_2;\ p_3^+ = \frac{1}{2}(z_{b1} + z_{b2});\ p_4^+ = \frac{1}{2}(\theta_{b1} - \theta_{b2});\ p_5^+ = \frac{1}{2}(x_{b1} - x_{b2}) \tag{15}$$

and the parameters of the antisymmetrical movements as

$$p_1^- = \theta_c;\ p_2^- = T_3;\ p_3^- = \frac{1}{2}(z_{b1} - z_{b2});\ p_4^- = \frac{1}{2}(\theta_{b1} + \theta_{b2});\ p_5^- = \frac{1}{2}(x_{b1} + x_{b2}). \tag{16}$$

Similarly, the following notations are used for the symmetrical excitation modes induced by the track nivelment irregularities

$$\eta_1^+ = \frac{1}{4}(\eta_1 + \eta_2 + \eta_3 + \eta_4); \quad \eta_2^+ = \frac{1}{4}(\eta_1 - \eta_2 - \eta_3 + \eta_4). \tag{17}$$

Unauthenticated
Download Date | 1/13/15 10:38 AM

For the antisymmetrical excitation modes, we have

$$\eta_1^- = \frac{1}{4}(\eta_1 + \eta_2 - \eta_3 - \eta_4); \quad \eta_2^- = \frac{1}{4}(\eta_1 - \eta_2 + \eta_3 - \eta_4). \tag{18}$$

Based on the symmetry and antisymmetry properties of the eigenfunctions of the first two vertical bending modes of the carbody $X_2(x)$ and $X_3(x)$, the below notations can be used

$$\varepsilon^+ = X_2(l_1) = X_2(l_2); \quad \varepsilon^- = X_3(l_1) = -X_3(l_2); \tag{19}$$

$$\lambda^+ = \frac{\mathrm{d}X_2(l_1)}{\mathrm{d}x} = -\frac{\mathrm{d}X_2(l_2)}{\mathrm{d}x}; \quad \lambda^- = \frac{\mathrm{d}X_3(l_1)}{\mathrm{d}x} = \frac{\mathrm{d}X_3(l_2)}{\mathrm{d}x}. \tag{20}$$

With the notations above, the system of 10 coupled equations is decomposed into two independent systems, five equations each. These systems describe the symmetrical and antisymmetrical movements of the vehicle, in the form of

$$\mathbf{M}^+\ddot{\mathbf{p}}^+ + \mathbf{C}^+\dot{\mathbf{p}}^+ + \mathbf{K}^+\mathbf{p}^+ = \mathbf{P}\dot{\boldsymbol{\eta}}^+ + \mathbf{R}\boldsymbol{\eta}^+; \tag{21}$$

$$\mathbf{M}^-\ddot{\mathbf{p}}^- + \mathbf{C}^-\dot{\mathbf{p}}^- + \mathbf{K}^-\mathbf{p}^- = \mathbf{P}\dot{\boldsymbol{\eta}}^- + \mathbf{R}\boldsymbol{\eta}^-, \tag{22}$$

where $\mathbf{p}^\pm = [\ p_1^\pm \quad p_2^\pm \quad p_3^\pm \quad p_4^\pm \quad p_5^\pm\ ]^{\mathrm{T}}$ represents the vector of the coordinates of the model's displacements and $\boldsymbol{\eta}^\pm = [\ \eta_1^\pm \quad \eta_2^\pm\ ]^{\mathrm{T}}$ – the vector of the symmetrical and antisymmetrical excitation modes.

The matrices $\mathbf{M}^+$ and $\mathbf{M}^-$ are the inertia matrices, in the below form

$$\mathbf{M}^+ = \mathrm{diag}(m_c, m_{m2}, m_b, J_b, m_b);$$

$$\mathbf{M}^- = \mathrm{diag}(J_c, m_{m3}, m_b, J_b, m_b).$$

The damping matrices, noted with $\mathbf{C}^+$ and $\mathbf{C}^-$, are written as

$$\mathbf{C}^+ = \begin{bmatrix} 4c_{zc} & 4c_{zc}\varepsilon^+ & -4c_{zc} & 0 & 0 \\ 4c_{zc}\varepsilon^+ & C_1 & -4c_{zc}\varepsilon^+ & 2C_2\lambda^+ & 4c_{xc}h_c\lambda^+ \\ -2c_{zc} & -2c_{zc}\varepsilon^+ & 2c_{zc} & 0 & 0 \\ 0 & C_2\lambda^+ & 0 & C_3 & 2c_{xc}h_b \\ 0 & 2c_{xc}h_c\lambda^+ & 0 & 2c_{xc}h_b & 2c_{xc} \end{bmatrix};$$

$$\mathbf{C}^- = \begin{bmatrix} C_4 & C_5 & -4c_{zc} & 2C_2 & 4c_{xc}h_c \\ C_5 & C_6 & -4c_{zc}\varepsilon^- & 2C_2\lambda^- & 4c_{xc}h_c\lambda^- \\ -2c_{zc}a_c & -2c_{zc}\varepsilon^- & 2c_{zc} & 0 & 0 \\ C_2 & C_2\lambda^- & 0 & C_3 & 2c_{xc}h_b \\ 2c_{xc}h_c & 2c_{xc}h_c\lambda^- & 0 & 2c_{xc}h_b & 2c_{xc} \end{bmatrix},$$

Unauthenticated
Download Date | 1/13/15 10:38 AM

by using the following notations:

$$C_1 = c_{m2} + 4c_{zc}(\varepsilon^+)^2 + 4(c_{xc}h_c^2 + c_{\theta c})(\lambda^+)^2;$$

$$C_2 = 2(c_{xc}h_c h_b - c_{\theta c}); \quad C_3 = 4c_{zb}a_b^2 + 2c_{xc}h_b^2 + 2c_{\theta c};$$

$$C_4 = 4(c_{zc}a_c^2 + c_{xc}h_c^2 + c_{\theta c}); \quad C_5 = 4[c_{zc}a_c\varepsilon^- + (c_{xc}h_c^2 + c_{\theta c})\lambda^-];$$

$$C_6 = c_{m3} + 4c_{zc}(\varepsilon^-)^2 + 4(c_{xc}h_c^2 + c_{\theta c})(\lambda^-)^2.$$

The matrices $\mathbf{K}^+$ and $\mathbf{K}^-$ are the stiffness matrices, under the form of

$$\mathbf{K}^+ = \begin{bmatrix} 4k_{zc} & 4k_{zc}\varepsilon^+ & -4k_{zc} & 0 & 0 \\ 4k_{zc}\varepsilon^+ & K_1 & -4k_{zc}\varepsilon^+ & 2K_2\lambda^+ & 4k_{xc}h_c\lambda^+ \\ -2k_{zc} & -2k_{zc}\varepsilon^+ & 2k_{zc} & 0 & 0 \\ 0 & K_2\lambda^+ & 0 & K_3 & 2k_{xc}h_b \\ 0 & 2k_{xc}h_c\lambda^+ & 0 & 2k_{xc}h_b & 2k_{xc} \end{bmatrix};$$

$$\mathbf{K}^- = \begin{bmatrix} K_4 & K_5 & -4k_{zc} & 2K_2 & 4k_{xc}h_c \\ K_5 & K_6 & -4k_{zc}\varepsilon^- & 2K_2\lambda^- & 4k_{xc}h_c\lambda^- \\ -2k_{zc}a_c & -2k_{zc}\varepsilon^- & 2k_{zc} & 0 & 0 \\ K_2 & K_2\lambda^- & 0 & K_3 & 2k_{xc}h_b \\ 2k_{xc}h_c & 2k_{xc}h_c\lambda^- & 0 & 2k_{xc}h_b & 2k_{xc} \end{bmatrix},$$

where $K_1 = k_{m2} + 4k_{zc}(\varepsilon^+)^2 + 4(k_{xc}h_c^2 + k_{\theta c})(\lambda^+)^2$;

$$K_2 = 2(k_{xc}h_c h_b - k_{\theta c}); \quad K_3 = 4k_{zb}a_b^2 + 2k_{xc}h_b^2 + 2k_{\theta c};$$

$$K_4 = 4(k_{zc}a_c^2 + k_{xc}h_c^2 + k_{\theta c}); \quad K_5 = 4[k_{zc}a_c\varepsilon^- + (k_{xc}h_c^2 + k_{\theta c})\lambda^-];$$

$$K_6 = k_{m3} + 4k_{zc}(\varepsilon^-)^2 + 4(k_{xc}h_c^2 + k_{\theta c})(\lambda^-)^2.$$

The vectors $\mathbf{P}$ and $\mathbf{R}$ are in the form of

$$\mathbf{P} = \begin{bmatrix} 0 & 0 & 4c_{zb} & 0 & 0 \\ 0 & 0 & 0 & 4c_{zb} & 0 \end{bmatrix}^{\mathrm{T}}; \quad \mathbf{R} = \begin{bmatrix} 0 & 0 & 4k_{zb} & 0 & 0 \\ 0 & 0 & 0 & 4k_{zb} & 0 \end{bmatrix}^{\mathrm{T}}.$$

The matrix equations (21) and (22) describe the dynamic behaviour of the vehicle in a mathematical manner, because of the vertical vibrations being excited by the track nivelment irregularities. These equations will be used for evaluating the carbody vibrations level and the identification of its critical points from the comfort perspective.

Unauthenticated
Download Date | 1/13/15 10:38 AM

3. The comfort index-based evaluation of the vibrating comfort

3.1. The power spectral density of the track irregularities

To evaluate the comfort in vertical vibrations, the track irregularities will be considered random and stationary. In these conditions, the power spectral density can be approximated by a theoretical curve, described by the equation [13]

$$S(\Omega) = \frac{A\Omega_c^2}{(\Omega^2 + \Omega_r^2)(\Omega^2 + \Omega_c^2)}, \tag{23}$$

where Ω is the wave number, $\Omega_c = 0.8246$ rad/m, $\Omega_r = 0.0206$ rad/m, and A is a constant that is a function of the track quality. For a better quality track, $A = 4.032 \cdot 10^{-7}$ radm is used; for a lower quality track, the constant A has the value of $1.080 \cdot 10^{-6}$ radm.

The track irregularities become an excitation factor for a vehicle that travels at speed V and this is the reason why the power spectral density of the track irregularities need to be expressed as a function of the angle frequency $\omega = V\Omega$,

$$G(\omega) = \frac{S(\omega/V)}{V}. \tag{24}$$

From equations (23) and (24), we have the power spectral density of the nivelment irregularity in the form of

$$G(\omega) = \frac{A\Omega_c^2 V^3}{[\omega^2 + (V\Omega_c)^2][\omega^2 + (V\Omega_r)^2]}. \tag{25}$$

3.2. The calculation of the comfort index

To evaluate the comfort in the vertical direction, the partial comfort index is used, which is calculated with the relation [10]

$$N_{MV} = 6a_{ZP95}^{W_{ab}}. \tag{26}$$

where a is the root mean square deviation of the vertical acceleration (Z) at the floor level (P), 95 refers to the quantile of order 95%, and $W_{ab} = W_a W_b$ represents the weight filter of the accelerations in the vertical direction.

The weight filter W_b, which takes into account the high human sensitivity to the vertical vibrations within the frequencies ranging from 5.6 to 13 Hz, has the transfer function in the form of

$$H_b(s) = \frac{(s + 2\pi f_3) \cdot \left[s^2 + \frac{2\pi f_5}{Q_3} s + (2\pi f_5)^2\right] 2\pi K f_4^2 f_6^2}{\left[s^2 + \frac{2\pi f_4}{Q_2} s + (2\pi f_4)^2\right]\left[s^2 + \frac{2\pi f_6}{Q_4} s + (2\pi f_6)^2\right] f_3 f_5^2}, \tag{27}$$

Unauthenticated
Download Date | 1/13/15 10:38 AM

where f_3 = 16 Hz, f_4 = 16 Hz, f_5 = 2.5 Hz, f_6 = 4 Hz, Q_2 = 0.63, Q_4 = = 0.8, K = 0.4 and $s = \mathrm{i}\omega$ (with $\mathrm{i}^2 = -1$).

The band pass filter W_a has the below transfer function

$$H_a(s) = \frac{s^2\,(2\pi f_2)^2}{\left[s^2 + \dfrac{2\pi f_1}{Q_1}s + (2\pi f_1)^2\right]\left[s^2 + \dfrac{2\pi f_2}{Q_1}s + (2\pi f_2)^2\right]}, \tag{28}$$

where f_1 = 0.4 Hz, f_2 = 100 Hz and Q_1 = 0.71.

When adopting the hypothesis that the vertical accelerations have a Gaussian distribution with the null mean value, the comfort index can be calculated with the equation

$$N_{MV}(x) = 6\Phi^{-1}(0.95)\sqrt{\frac{1}{\pi}\int_0^\infty \omega^4 G(\omega)\left|\bar{H}_c(x,\omega)\right|^2\left|\bar{H}_{ab}(\omega)\right|^2 \mathrm{d}\omega}, \tag{29}$$

where $\Phi^{-1}(0.95)$ represents the quantile of the standard Gaussian distribution with the probability of 95%, $\bar{H}_c$ – the response factor of the vehicle carbody, and $\bar{H}_{ab}$ is the weight factor of the W_{ab} filter.

The response factor in a point x of the carbody is in the form of

$$\bar{H}_c(x,\omega) = \bar{H}_{z_c}(\omega) + \left(\frac{L}{2} - x\right)\bar{H}_{\theta_c}(\omega) + \sum_{n=2}^{3} X_n(x)\bar{H}_{T_n}(\omega), \tag{30}$$

where $\bar{H}_{z_c}(\omega)$, $\bar{H}_{\theta_c}(\omega)$, $\bar{H}_{T_i}(\omega)$ are the response factors corresponding to the rigid vibration modes – bounce (z_c) and pitch (θ_c), and also to the natural bending modes of the carbody – symmetrical (T_2) and antisymmetrical (T_3), that can be calculated via the equations

$$\bar{H}_{z_c}(\omega) = \frac{\bar{P}_1^+}{\bar{\eta}_0}; \quad \bar{H}_{\theta_c}(\omega) = \frac{\bar{P}_1^-}{\bar{\eta}_0}; \quad \bar{H}_{T_2}(\omega) = \frac{\bar{P}_2^+}{\bar{\eta}_0}; \quad \bar{H}_{T_3}(\omega) = \frac{\bar{P}_2^-}{\bar{\eta}_0}. \tag{31}$$

4. Numerical application

The section below includes the results in the numerical simulations derived from the previously presented model and the method. The reference parameters of the model are shown in Table 1.

Figure 2 displays the vertical comfort index calculated in the carbody reference points – at the centre and above the two bogies, while travelling at speeds of up to 300 km/h on a track whose quality is described by the constant $A = 1.080 \cdot 10^{-6}$ radm.

Unauthenticated
Download Date | 1/13/15 10:38 AM

Table 1.

The model reference parameters

m_c = 34000 kg	$4k_{zc}$ = 2.4 MN/m
m_b = 3200 kg	$2k_{xc}$ = 340 kN/m
J_c = 1963840 kg·m^2	$2k_{\theta c}$ = 256 kN/m
J_b = 2048 kg·m^2	$4c_{zc}$ = 68.88 kNs/m
EI = 3.2·10^9 Nm^2	$2c_{xc}$ = 50 kNs/m
m_{m2} = 35224 kg	$2c_{\theta c}$ = 2 kNm
m_{m3} = 33950 kg	c_{m2} = 53.469 kNm/s
L = 26.4 m	c_{m3} = 142.052 kNm/s
$2a_c$ = 19 m	$4k_{zb}$ = 4.4 MN/m
$2a_b$ = 2.56 m	$4c_{zb}$ = 52.21 kNs/m
h_c = 1.3 m	k_{m2} = 90.182 MN/m
h_b = 0.2 m	k_{m3} = 660.415 MN/m

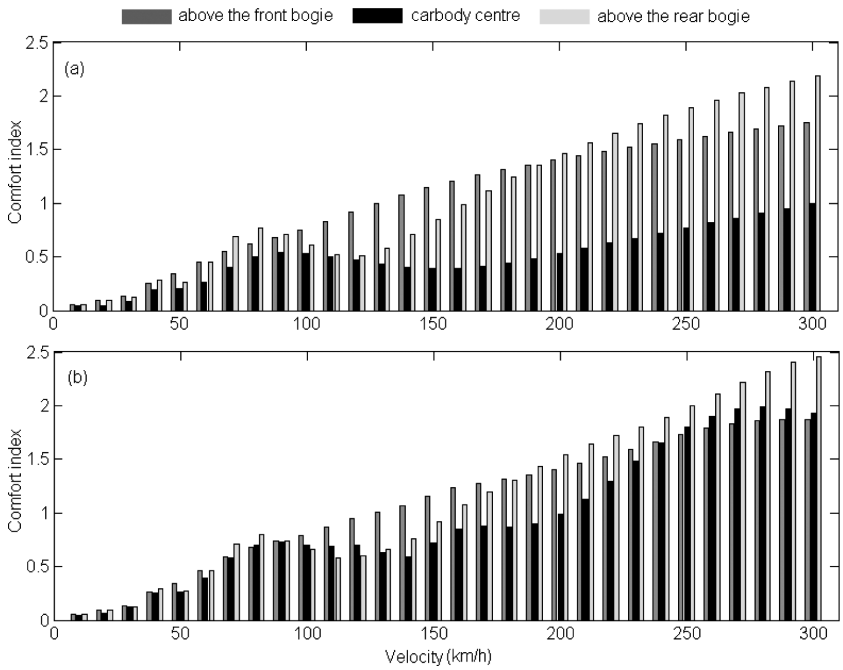

Fig. 2. The position of the critical point of the vibrations level, depending on the running behaviour: (a) „the rigid carbody" model; (b) the „flexible carbody" model

On the one hand, the vibrations behaviour does not continually intensify along with the velocity, because of the geometric filtering effect of the

Unauthenticated
Download Date | 1/13/15 10:38 AM

nivelment irregularities [12]. This effect can be more noticed at the carbody centre, where the filtering effect takes place due to the carbody wheelbase, and also the filtering effect from the bogie wheelbase. In the reference points above the bogies, the geometric filtering effect is visibly lower because this is the location where only the geometric filtering takes place, coming from the distance between the bogie axles. On the other hand, there can be noticed the different vibrations behaviour of the carbody in the reference points above the two bogies, which is possible from the damping of the vertical suspension and also from the geometric filtering effect [14].

Should the carbody structural vibrations are not taken into account, and this is modelled as a rigid body (diagram a), the derived results show that the comfort index at the carbody centre is always smaller than the one against the two bogies, and differences increase along the velocity. Hence, the critical point of the vibrations level is found – depending on the running behaviour – either above the front bogie or above the rear one.

The results derived from the insertion into the vehicle model of the carbody flexible vibration modes (diagram b) differ both qualitatively and quantitatively from those described in the diagram (a). It can be noticed that the level of vibrations at the carbody centre is much higher than the one evaluated on the basis of „rigid carbody" model and it is comparable to the one calculated in the reference points above those two bogies. Moreover, the comfort index at the carbody centre is higher than the one above the front bogie, for velocities between 250 and 300 km/h. The quantity differences are displayed via the errors represented in the diagrams in Fig. 3. Thus, it is obvious that the neglect of the carbody flexible vibration modes will lead to errors smaller than 10% (diagram a) and 16% (diagram c), respectively for the comfort index calculated in the carbody reference points above the two bogies. On the contrary, the model error is significant at the carbody centre, being able to reach 57% (diagram b). In spite of this, the critical point of the carbody vibrations level remains the same in the reference point above one of the bogies, irrespective of the running behaviour.

For the carbody with high bending stiffness, the results obtained from the „flexible carbody" model and from the „rigid carbody" model sometimes become comparable or even equal. This is evident in Fig. 4, which features the comfort index calculated at the speed of 250 km/h in all three carbody reference points for values of EI between 10^9 and 10^{10} Nm^2. According to the diagrams (a) and (c), the level of vibrations in the reference points above the two bogies does not practically depend on the parameter called the elasticity module, if higher than a certain value. Thus, the comfort index above the bogies will become equal with the comfort index calculated by the application of the „rigid carbody" model, should the carbody bending

Unauthenticated
Download Date | 1/13/15 10:38 AM

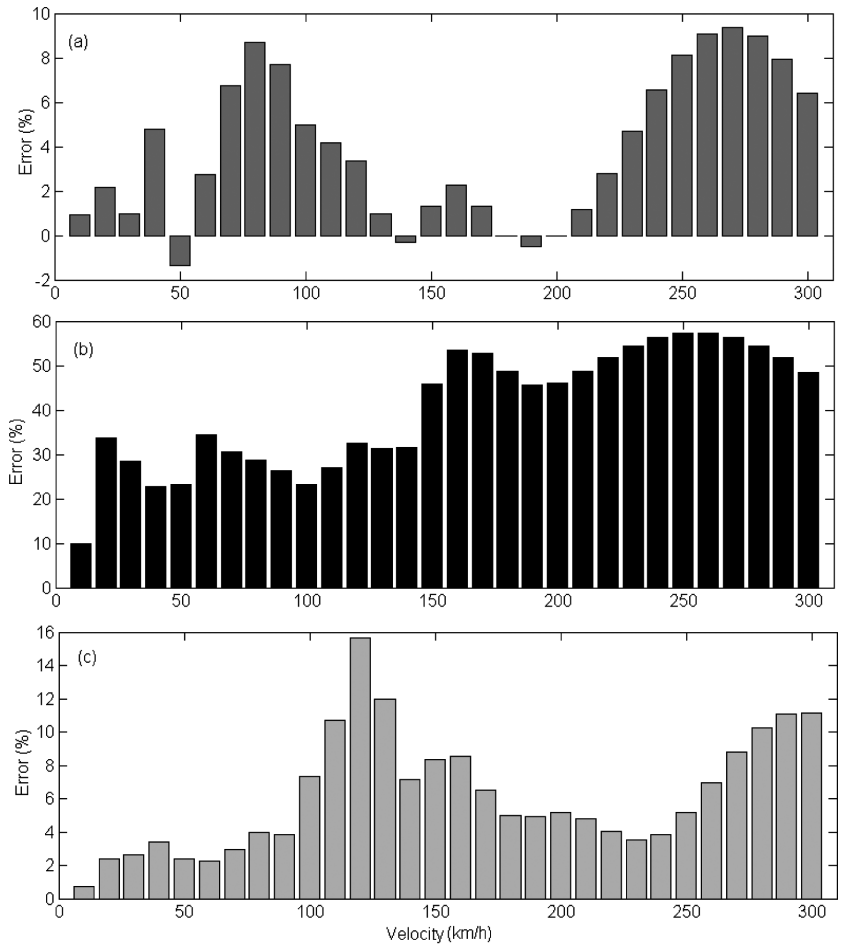

Fig. 3. The model error:
(a) above the front bogie; (b) carbody centre; (c) above the rear bogie

module is higher than $4 \cdot 10^9$ Nm^2. At the carbody centre (diagram b), the decrease in the level of vibrations while the bending module is higher is more pronounced above the bogies and the dependence on this parameter is present throughout all the range of values being considered. This is the reason why there are differences between the results derived from the „flexible carbody" model and from the „rigid carbody" model, even for high values of *EI*. These differences significantly lower, from circa 60% (for $EI = 10^9$ Nm^2) to 10% (for $EI = 10^{10}$ Nm^2).

As further shown, the modification of the parameters of the vertical suspension can lead to the migration of the critical point of the vibrations level in the carbody from one reference point to another, and this can be only highlighted by the implementation of the „flexible carbody" model.

Unauthenticated
Download Date | 1/13/15 10:38 AM

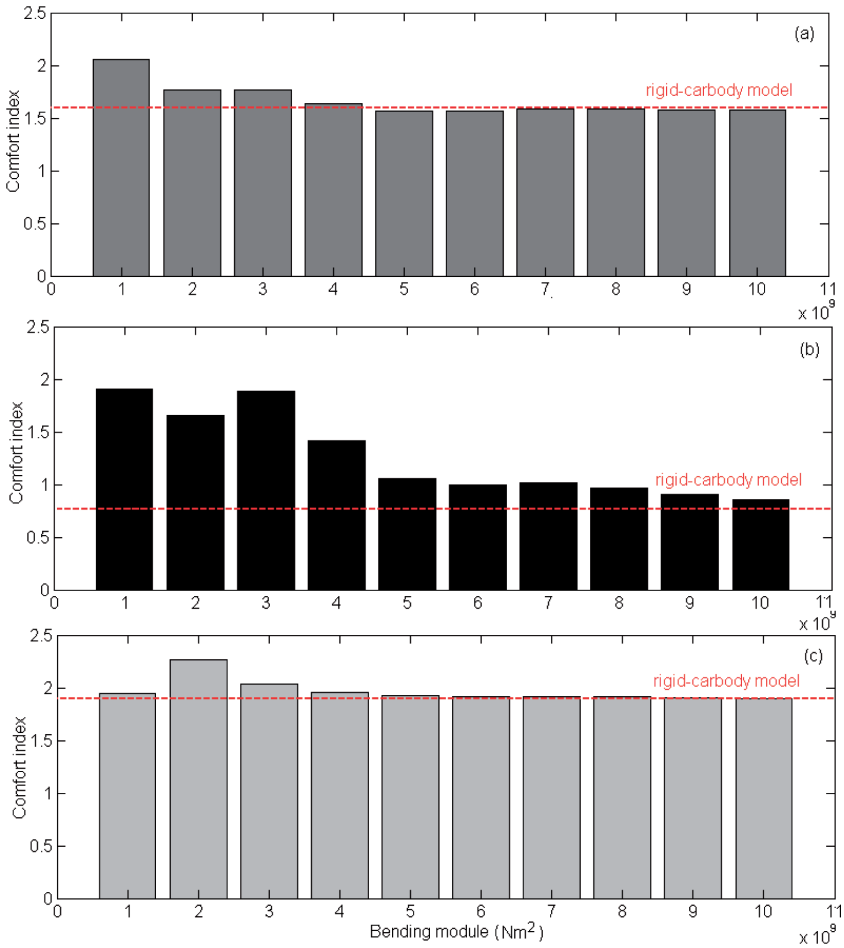

Fig. 4. The influence of the carbody bending module upon the carbody vibrations level at speed of 250 km/h: (a) above the front bogie; (b) carbody centre; (c) above the rear bogie

To simplify the analysis, the damping degrees corresponding to the two suspension stages are being introduced, as below

$$\zeta_c = \frac{4c_{zc}}{2\sqrt{4k_{zc}m_c}}; \quad \zeta_b = \frac{4c_{zb}}{2\sqrt{4k_{zb}m_b}}. \tag{32}$$

Based on the diagrams in Fig. 5, the position of the critical point is being examined, as a function of the damping degree of the secondary suspension, at the speed of 250 km/h. According to the diagram (a), which features the results from the „rigid carbody" model, the critical point is above the rear bogie, for a secondary suspension damping lower than 0.3. Should the

Unauthenticated
Download Date | 1/13/15 10:38 AM

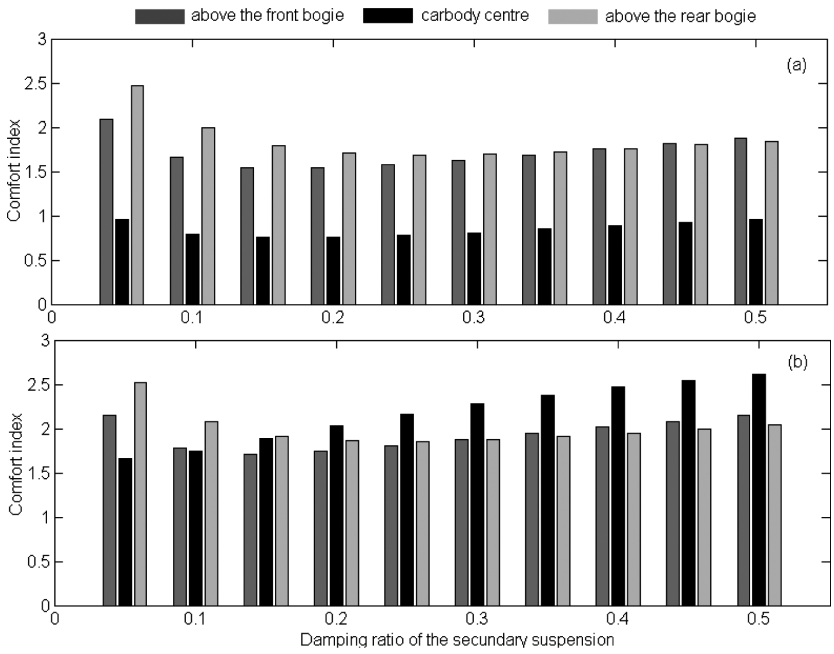

Fig. 5. The position of the critical point at 250 km/h depending on the damping ratio of the secondary suspension: (a) „rigid carbody" model; (b) „flexible carbody" model

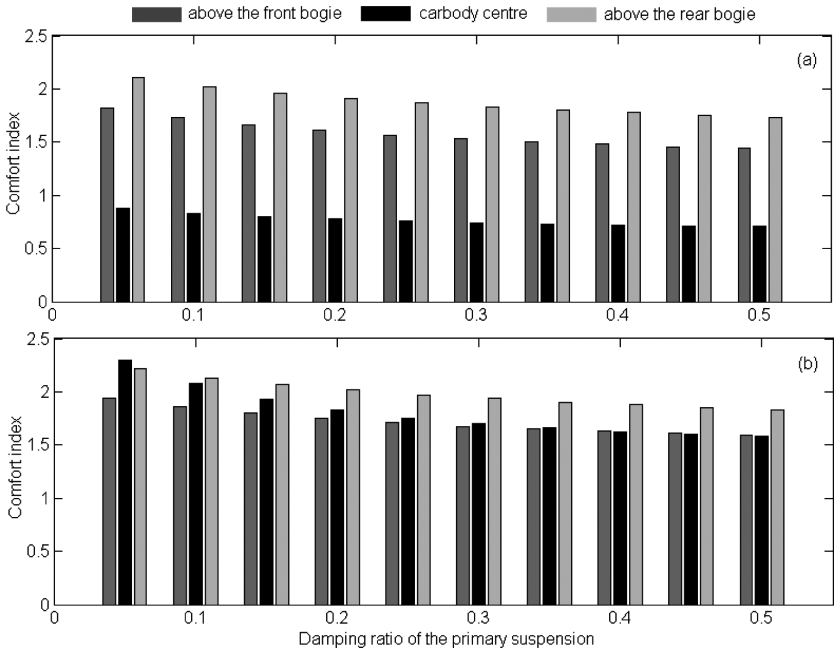

Fig. 6. The position of the critical point at 250 km/h depending on the damping ratio of the primary suspension: (a) „rigid carbody" model; (b) „flexible carbody" model

Unauthenticated
Download Date | 1/13/15 10:38 AM

damping increases continually, the level of vibrations above the two bogies tends to become equal. The results in diagram (b), derived from the „flexible carbody" model, show that the critical point shifts from the rear bogie towards the carbody centre, should the damping degree of the secondary suspension is higher than 0.2.

Should the position of the critical point of the carbody at 250 km/h for various damping ratios of the primary suspension based on the „rigid carbody" model is being examined (Fig. 6, diagram a), this point can be noticed to remain above the rear bogie for all the cases under study. While using the „flexible carbody" model (Fig. 6, diagram b), it becomes evident that the critical point is at the carbody centre for low damping of the primary suspension ($\zeta_b = 0.05$), and the increase of the damping will make this point move above the rear bogie. It can be noticed that the comfort index at the carbody centre has a high value for the entire range of damping values, close to the one calculated above the bogies.

5. Conclusions

The simple models represent useful research instruments to explain certain basic phenomena in the vibrations behaviour of the railway vehicles. When the issue of evaluating the vehicle dynamic performance to have trustworthy quantity results arises, it is necessary to adopt certain complex models that will consider important factors affecting the level of vibrations in the vehicle.

The comfort performance of the railway vehicle evaluated on the basis of a „rigid carbody" model is overestimated, compared to the results from the implementation of a „flexible carbody" model. For the carbodies with a high bending flexibility, the model errors are significant, mainly at the carbody centre, where the comfort index calculated with the „rigid carbody" model can be circa three times smaller, at high velocities. In this reference point, differences of at least 10% between the comfort index calculated with the „rigid carbody" model and the one with „flexible carbody" model are maintained, even for the carbodies with a high bending rigidity.

From the comfort perspective, the results derived from the neglect of the carbody vibration flexible modes show that the critical points of the carbody vibrations level is above one of the bogies, irrespective of the speed behaviour. Upon applying the „flexible carbody" model, the comfort index at the carbody centre is shown to be comparable to the one above the bogies. Moreover, under certain conditions – high damping of the secondary suspe-

Unauthenticated
Download Date | 1/13/15 10:38 AM

nion or a low damping of the primary suspension – the critical point of the vibrations level shifts from above the bogie to the carbody centre.

Manuscript received by Editorial Board, July 23, 2014;
final version, September 28, 2014.

REFERENCES

[1] Sebeşan I., Mazilu T.: Vibraţiile vehiculelor feroviare (Vibrations of the railway vehicles), Matrixrom, Bucureşti, 2010.
[2] Carlbom P.: Carbody and Passengers in Rail Vehicle Dynamics, Ph.D. Thesis, Division of Railway Technology, Department of Vehicle Engineering, Royal Institute of Technology, Stockholm, Sweden, 2000.
[3] Diana G., Cheli F., Collina A., Corradi R., Melzi S.: The development of a numerical model for railway vehicles comfort assessment through comparison with experimental measurements, Vehicle System Dynamics, 2002, Vol. 38, No. 3, pp. 165-183.
[4] Cheli F., Corradi R.: On rail vehicle vibrations induced by track unevenness: Analysis of the excitation mechanism, Journal of Sound and Vibration, 2011, Vol. 330, pp. 3744-3765.
[5] Zhou J., Goodall R., Ren L., Zhang H.: Influences of car body vertical flexibility on ride quality of passenger railway vehicles, Proceedings of the Institution of Mechanical Engineers, Part F: Journal of Rail and Rapid Transit, 2009, Vol. 223, pp. 461-471.
[6] Zhou J., Wenjing S.: Analysis on geometric filtering phenomenon and flexible car body resonant, Vibration of Railway Vehicles, Journal of Tongji University, Natural Science, 2009, Vol. 37, Iss. 12, pp. 1653-1657.
[7] Dumitriu M.: Evaluation of the comfort index in railway vehicles depending on the vertical suspension, Annals of Faculty Engineering Hunedoara – International Journal of Engineering, 2013, Tome XI, Fascicule 4, pp. 23-32.
[8] Dumitriu M.: Influence of the suspension damping on ride comfort of passenger railway vehicles, UPB Scientific Bulletin, Series D: Mechanical Engineering, 2012, Vol. 74, Iss. 4, pp. 75-90.
[9] Tomioka T., Takigami T., Suzuki Y.: Numerical analysis of three-dimensional flexural vibration of railway vehicle car body, Vehicle System Dynamics, 2006, Vol. 44, Supplement, pp. 272-285.
[10] ENV 12299, Railway applications ride comfort for passengers measurement and evaluation, 1997.
[11] UIC 513 R, Guidelines for evaluating passenger comfort in relation to vibration in railway vehicle, International Union of Railways, 1994.
[12] Dumitriu M.: Influence of the vertical suspension on the vibration behavior in the railway vehicles, Annals of the University of Petroşani, Mechanical Engineering, 2011, Vol. 13, pp. 35-50.
[13] C 116, Interaction between vehicles and track, RP 1, Power spectral density of track irregularities, Part 1: Definitions, conventions and available data, Utrecht, 1971.
[14] Dumitriu M.: Geometric filtering effect of vertical vibrations of railway vehicles, Analele Universităţii "Eftimie Murgu" Resiţa, 2012, No. 1, pp. 48-61.

Unauthenticated
Download Date | 1/13/15 10:38 AM

O punktach krytycznych drgań pionowych w pojeździe szynowym

S t r e s z c z e n i e

W artykule oceniono poziom drgań pionowych w nadwoziu pojazdu szynowego generowanych przez nierówności toru i zbadano położenie punktu krytycznego z punktu widzenia komfortu jazdy. Zagadnienie jest rozważane na podstawie zarówno modelu ”nadwozia sztywnego”, jak modelu ”nadwozia elastycznego”, który wykorzystuje dwa pierwsze modele ugięcia nadwozia. Wyznaczono błędy modelu w funkcji prędkości jazdy, a wyniki obliczeń dowodzą, że parametry komfortu jazdy pojazdu szynowego, oceniane na podstawie modelu ”nadwozia sztywnego”, są zawyżone w porównaniu z tymi, jakie uzyskuje się przy zastosowaniu modelu ”nadwozia elastycznego”, zwłaszcza dla środkowej części nadwozia. Pokazano jednocześnie, że poprawna estymacja punktu krytycznego dla poziomu drgań wymaga modelowania drgań strukturalnych nadwozia pojazdu.

Unauthenticated
Download Date | 1/13/15 10:38 AM